AIP | Review of Scientific Instruments

Dispersion interferometer using modulation amplitudes on LHD (invited)a)

T. Akiyama, R. Yasuhara, K. Kawahata, S. Okajima, and K. Nakayama

Citation: Review of Scientific Instruments **85**, 11D301 (2014); doi: 10.1063/1.4886777

View online: http://dx.doi.org/10.1063/1.4886777

View Table of Contents: http://scitation.aip.org/content/aip/journal/rsi/85/11?ver=pdfcov

Published by the AIP Publishing

Dispersion interferometer using modulation amplitudes on LHD (invited)[a)]

T. Akiyama,[1,b)] R. Yasuhara,[1] K. Kawahata,[1] S. Okajima,[2] and K. Nakayama[2]
[1]*National Institute for Fusion Science, 322-6 Oroshi-cho, Toki-shi, Gifu 509-5292, Japan*
[2]*Chubu University, Matsumoto-cho, Kasugai-shi, Aichi 487-8501, Japan*

(Presented 2 June 2014; received 30 May 2014; accepted 23 June 2014; published online 14 July 2014)

Since a dispersion interferometer is insensitive to mechanical vibrations, a vibration compensation system is not necessary. The CO_2 laser dispersion interferometer with phase modulations on the Large Helical Device utilizes the new phase extraction method which uses modulation amplitudes and can improve a disadvantage of the original dispersion interferometer: measurement errors caused by variations of detected intensities. The phase variation within $\pm 2 \times 10^{17}$ m^{-3} is obtained without vibration compensation system. The measured line averaged electron density with the dispersion interferometer shows good agreement with that with the existing far infrared laser interferometer. Fringe jump errors in high density ranging up to 1.5×10^{20} m^{-3} can be overcome by a sufficient sampling rate of about 100 kHz. © *2014 AIP Publishing LLC*. [http://dx.doi.org/10.1063/1.4886777]

I. INTRODUCTION

Electron density measurement with an interferometer is indispensable on present fusion devices for both device operation and physics study. Especially for future fusion reactors, high density resolution with high reliability (no measurement failures) is required for safe operation. As a density measurement method, an interferometer is mainly utilized on most fusion devices. However, the mechanical vibrations cause measurement errors for the interferometer and a fringe jump error in the high density range leads to uncontrollability of the density. Hence, great efforts have been paid for the development of the electron density measurement which overcomes the above limitations of the interferometer.

One of the candidate methods is a polarimeter which measures the electro-magnetic interactions between a plasma and waves such as the Faraday effect[1–3] and the Cotton-Mouton effect.[4,5] The vibration isolation system is not necessary for a polarimeter since the changes in the polarization do not depend on the change in the optical path length caused by mechanical vibrations. The reason for the fringe jump error of the interferometer is as follows: the measured phase shift corresponds to several density values due to uncertainty of 2π when the phase shift is larger than one fringe. The change in the polarization and the ellipticity angles is usually smaller than one period for the wavelength of present lasers.

The feasibilities of the density measurement based on the polarimeter have been already proven on the several large fusion devices.[1–5] These interactions depend upon not only the electron density but also the magnetic field strength. The dependence on the magnetic field is an advantage because information such as the magnetic fluctuations can be obtained. On the other hand, the dependence on the magnetic field is also a disadvantage because the dependence makes the density evaluation complicated and the precise magnetic field strength for a high density resolution is necessary.

The other method is a dispersion interferometer (DI).[6–13] As shown below, a dispersion interferometer is also insensitive to the mechanical vibrations. Since the measurement errors caused by the vibrations are small, the phase shift due to a plasma less than one fringe would be acceptable. Then the DI is principally free from the fringe jump error by selecting the short wavelength of the laser because the electron density can be determined from the phase shift without uncertainty of 2π.

The DI was firstly used for measurement of contour of the semiconductor surface in the 1980s.[6,7] It was applied for the electron density measurement of fusion plasmas on the linear device GDI[8] in the 1990s and TEXTOR tokamak in the 2000s.[9,11] These days, the DI has been installed on a FRC[10] and a helical device.[13] It will be installed on W7-X[14] and is one of the candidates for the electron density measurement on ITER.[15] As a versatile application, the DI is also attractive for the electron density measurement of an atmospheric-pressure plasma because the DI can significantly reduce the phase shift caused by a change in the gas-pressure, which is cancelled as the same as the mechanical vibrations, during the discharge.[16]

The original DI is basically a homodyne interferometer. The limitations of the homodyne interferometer are common to the DI: (1) restriction of the measurable range of the phase shift within a monotonic function of the interference signal (a cosine function), less than up to π, and (2) measurement errors caused by changes in the detected intensity of an interference signal. The detected intensities tend to vary during plasma discharges by refraction of the probe beam in a plasma, instabilities of laser oscillation, and electromagnetic noises. In order to resolve the former limitation (1), the phase modulation is introduced and the dynamic range up to 2π is expanded.[9] In addition to the phase modulation, the phase extraction method from the ratios of modulation amplitudes[12]

[a)]Invited paper, published as part of the Proceedings of the 20th Topical Conference on High-Temperature Plasma Diagnostics, Atlanta, Georgia, USA, June, 2014.

[b)]Author to whom correspondence should be addressed. Electronic mail: takiyama@lhd.nifs.ac.jp

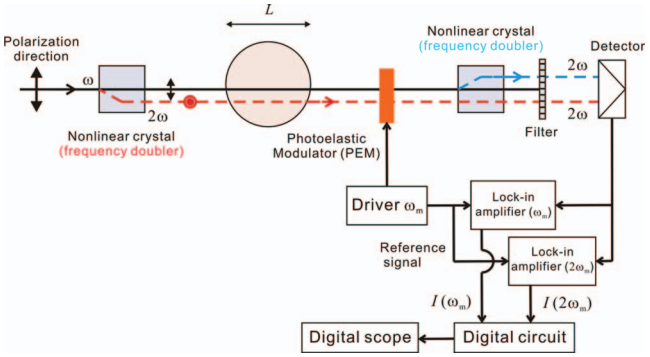

FIG. 1. Optical and electronic arrangements of the phase modulated dispersion interferometer which uses a ratio of modulation amplitudes for phase extraction.

can also extend the dynamic range up to 2π and can resolve the latter limitation (2).

In this paper, the optical system and its performance of the DI installed on the Large Helical Device (LHD), which uses the phase modulation and the phase extraction method from the ratio of modulations amplitudes, are described. Section II roughly shows the principle of the DI which uses the ratio of modulation amplitudes. The optical system on LHD is mentioned in Sec. III. The measurement results are shown in Sec. IV. Section IV gives discussion and Sec. V summarizes.

II. PRINCIPLE OF PHASE EXTRACTION METHOD

Since the principle of the phase extraction method is described in Ref. 12 in detail, only the essence is shown here. The probe beam of the DI is a mixture of the fundamental and the second harmonic beams, which is generated with a nonlinear crystal, as shown in Fig. 1. The beam paths of these two beams are almost the same and the mechanical vibrations are common. The polarization of these two beams is perpendicular to each other. After passing through a plasma and a following phase modulator, another second harmonic beam is generated with another nonlinear crystal. Here, the photoelastic modulator (PEM), whose drive direction is set to be parallel to the polarization direction of the second harmonic beam, is used to modulate only the second harmonics beam. The residual fundamental beam is filtered out and the interference between the two second harmonic beams is detected.

In the case of the conventional DI, the interference signal is

$$I(t) = A + B\cos\left(\frac{3}{2}\frac{c_p\bar{n}_e L}{\omega} + \phi\right), \quad (1)$$

where A and B are $I_1 + I_2$ and $\sqrt{I_1 I_2}$, respectively, which are determined by the detected intensities I_1 and I_2 of the second harmonic beams. $\bar{n}_e$ and L are the line averaged electron density and the optical path length in a plasma, respectively. ω is the frequency of the laser beam and c_p is the constant. ϕ is an initial phase. In order to evaluate the phase shift which is proportional to the electron density, A and B are necessary. These values are evaluated from a calibration experiment without plasma. However, if the detected intensity varies during plasma discharges, the density error is included in the evaluated electron density, as illustrated in Fig. 2, because the electron density is directly evaluated from the intensity signal. On the other hand, the phase modulated interference signal is given as follows:

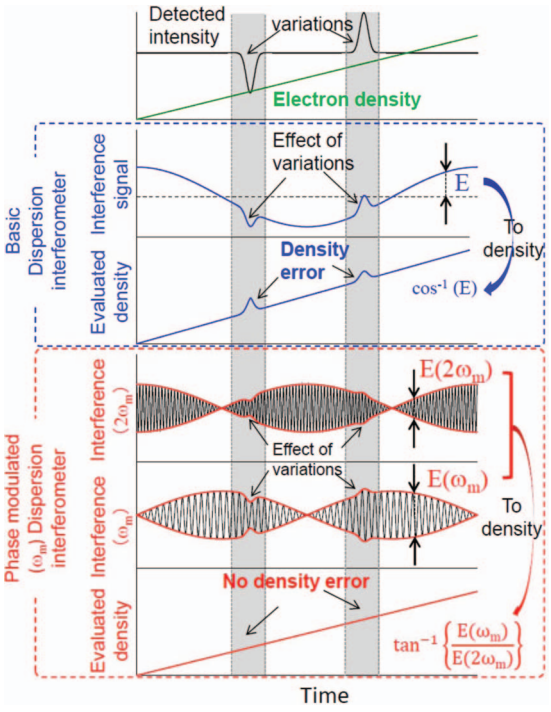

FIG. 2. Comparison of the phase extraction methods between the basic dispersion interferometer and the phase modulated dispersion interferometer which uses a ratio of modulation amplitudes. Here, two intensity variations appear during density ramp-up.

$$I(t) = A + B\cos\left(2\rho_0 \sin\omega_m t + \frac{3}{2}\frac{c_p\bar{n}_e L}{\omega} + \phi\right). \quad (2)$$

ρ_0 is the optical retardation given by the PEM and ω_m is the drive frequency. Equation (2) consists of the harmonics of the drive frequency ω_m. The amplitudes of the fundamental I_{ω_m} and the second harmonics $I_{2\omega_\mathrm{m}}$ are given by

$$I_{\omega_m} = -2BJ_1(2\rho_0)\sin\left(\frac{3}{2}\frac{c_p\bar{n}_e L}{\omega} + \phi\right), \quad (3)$$

$$I_{2\omega_m} = 2BJ_2(2\rho_0)\cos\left(\frac{3}{2}\frac{c_p\bar{n}_e L}{\omega} + \phi\right), \quad (4)$$

where J_1 and J_2 are the Bessel function of order of the first and the second. The line averaged density is evaluated from the following expression:

$$\bar{n}_e = -\frac{2}{3}\frac{\omega}{c_p L}\left\{\tan^{-1}\left(\frac{I_{\omega_m}}{I_{2\omega_m}}\right) + \phi\right\}. \quad (5)$$

Here, $\rho_0 = 1.3$ rad. for $J_1(2\rho_0) = J_2(2\rho_0)$. As shown in Fig. 2, the envelopes of the fundamental and the second harmonic components vary due to the intensity variations. However, by using the ratio of the amplitudes, the variations are canceled in the electron density evaluation. Therefore, this method is free from variations of detected intensities, which is one of the error sources of the dispersion interferometer.

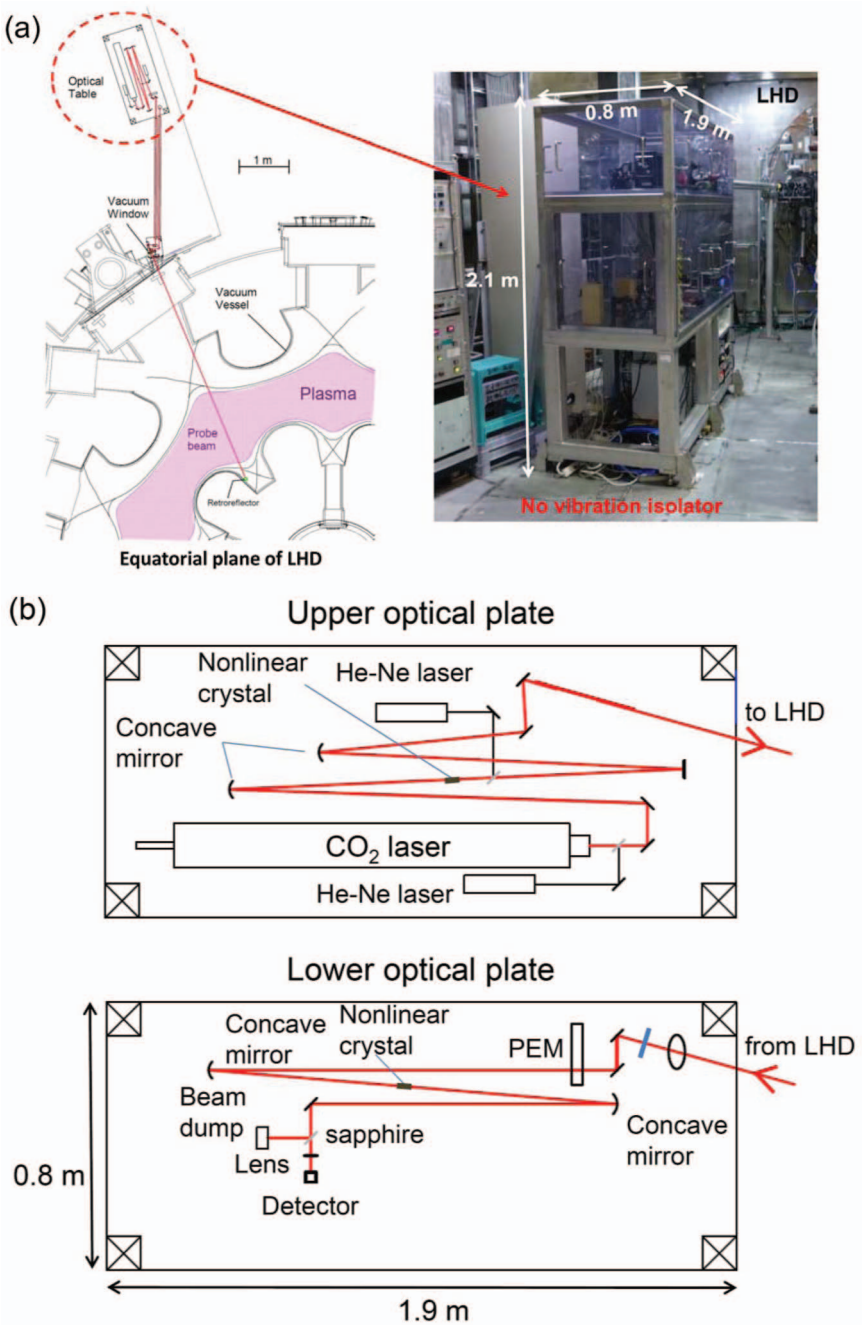

FIG. 3. (a) Layout of the optical table for the dispersion interferometer in the equatorial plane of the LHD hall and a photograph of the optical bench. (b) Arrangements of optical components on optical tables in the bench.

III. OPTICAL SETUP OF BENCH TESTING

Figure 3(a) shows the layout of the optical bench, where optical components are placed in the LHD experiment hall and a photograph of the bench. The optical bench is installed on the floor without a vibration isolation system. The bench is bi-level and arrangements of the optical components are shown in Fig. 3(b). The frequency-stabilized CO_2 laser (GN-802-GES, MPB Technology) whose wavelength is 10.6 μm, the first nonlinear crystal $AgGaSe_2$ (Crystech Inc.) with a dimension of 5 × 5 × 15 mm, and focusing mirrors are placed on the upper optical plate as shown in Fig. 3(b). The CO_2 laser light is focused on the nonlinear crystal to increase the power density, which can increase the efficiency of the second harmonic generation. The output power of the CO_2 laser is about 7 W and that of the generated second harmonic is about 50 μW. The nonlinear crystals are air-cooled with fans and the temperature rise is less than about 10 °C. Even if there are no fans, the temperature rise is about 20 °C. This is due to the small absorption coefficient. Some optics, such as mirrors to inject the laser beam into LHD, are fixed directly to the port of LHD. The laser beam is injected from the outboard side to the inboard side and is reflected by a retroreflector made of 316 stainless steel installed inside the LHD vacuum vessel. The beam radius of the fundamental component along

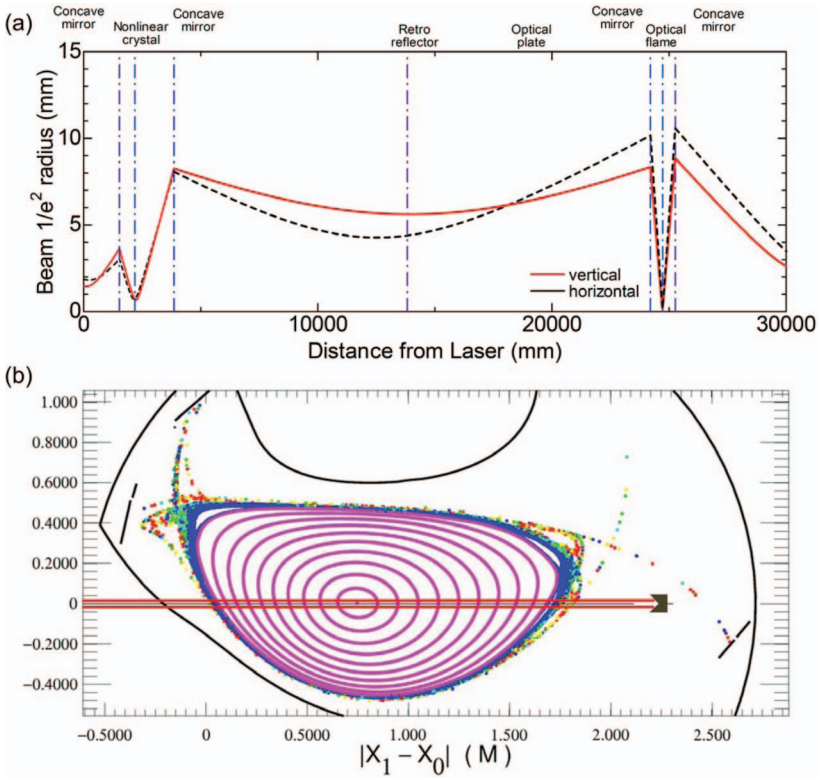

FIG. 4. (a) Distributions of the $1/e^2$ beam radius of horizontal and vertical directions along the optical beam path. (b) The line of sight of the dispersion interferometer and plasma cross section (radial position of the magnetic axis is 3.60 m).

the beam path is shown in Fig. 4(a). A beam waist of the fundamental beam is about 5 mm and is located at the position of the retroreflector. The laser beam paths are displaced ±15 mm vertically from the equatorial plane to separate the back and forth beams. The beam path and the cross section of the LHD plasma are illustrated in Fig. 4(b). The back beam goes to the optical bench again. The phase of the second harmonics beam is modulated with the PEM (II/ZS50, Hinds Instruments) with a drive frequency of 50 kHz. The other second harmonics beam is generated with the second nonlinear crystal (ELAN Inc.). A sapphire plate cuts the fundamental beam and the interference between the two second harmonic beams is detected with a paltrier cooling detector (PVI-3TE-5, VIGO). The amplitudes of fundamental and second harmonic components of the drive frequency are obtained with lock-in amplifiers, which are typically operated with a time constant of 30 μs. The phase differences between the modulation signals and the drive signal to the PEM are also detected with the lock-in amplifier to identify the quadrant, and they are digitized. By detecting the quadrant, the phase shift can be determined uniquely up to 2π.

IV. EXPERIMENT RESULTS

Figures 5(a) and 5(b) show the variations of the baseline of the line averaged electron density for short and long times, respectively. Despite no vibration compensation system and direct attachment of the optical components to LHD, the width of the variation for 3 s, which is the typical discharge duration time, is about $\pm 2 \times 10^{17}$ m^{-3} in the case of a path length in a plasma and is 3.28 m for double path. This small variation of the baseline indicates that the phase shift due to the mechanical vibrations is well cancelled. The remaining variations might come from the following reasons. One is the uncanceled vibration components. If there is large displacement of the optical axis between the fundamental and the second harmonic beams, the cancellation

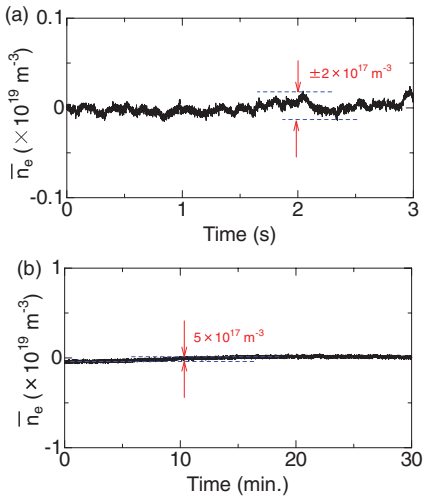

FIG. 5. (a) Variations of the evaluated line averaged electron density. The width of the variation is within $\pm 2 \times 10^{17}$ m^{-3} for typical LHD discharge duration. (b) The drift of the baseline for 30 min.

might be imperfect. The wavefront should be overlapped completely. The walk-off in the nonlinear crystal and window material causes the beam displacement of around 0.1 mm. A wedge plate which can change the direction of the beam axis may reduce the baseline variations. Similar to that, the distortion of the wavefronts, which is due to multi-reflection in the window material or the PEM, also causes the imperfections of vibration cancellation. One of the solutions is an adaptive optics, which consists of a wavefront sensor and a deformable mirror. As for long time measurement, observed slow variations are speculated to be related to changes in the room temperature. The temperature variations might change the optical constant of some optical components.

The electron density of an atmospheric-pressure plasma, whose density response is almost the same (within several μs) as that of the discharge current was conducted, in order to evaluate the actual temporal response of the DI. The plasma source was placed just in front of the PEM and the laser beam is focused on the micro plasma[16] by adding lenses. From the measurements, it is found that there is a delay time of about 80 μs in the evaluated density compared with the actual density rise. The time constant of the evaluated density is about 100 μs in the case of a time constant of the lock-in amplifier of 30 μs. These characteristics of the responses are expected to come from the lock-in amplifiers. The digital lock-in technique, which has been adopted in the MSE,[17] would improve the time response of the DI.

Measurement results of LHD plasma with the DI and the existing far infrared laser interferometer are shown in Figs. 6(a) and 6(b). Although the lines of sight are different from each other (FIR: vertical line of sight, DI: horizontal line of sight), they show good agreement. One of the possible reasons for the about 5% averaged difference between the DI and the far infrared laser interferometer, shown in Fig. 6(c), is an error of the optical path length in a plasma. The optical path lengths are defined as the distance inside the last closed magnetic surface (LCFS) which is determined by equilibrium calculations. However, the density of the LHD plasma actually expands to the stochastic layer outside the LCFS and the expansion is different at each cross section. The modulation of the evaluated density with the DI $\Delta n_e = n_e^{Dis} - 0.96 \times n_e^{FIR}$ of an amplitude of $\pm 2 \times 10^{18}$ m^{-3}, is seen as shown in Fig. 6(c). This modulation is caused by offsets included in the amplitudes of the modulation I_{ω_m}, $I_{2\omega_m}$ for the density evaluation. Supposing that the offsets C and D are added to the amplitude signals,

$$I_{2\omega_m} = 2BJ_2(2\rho_0)\cos(\psi) + C,$$
$$I_{\omega_m} = -2BJ_1(2\rho_0)\sin(\psi) + D.$$

Then the additional modulation term appears in the evaluated phase shift ψ':

$$\psi' = \tan^{-1}(I_{\omega_m} / I_{2\omega_m}) = -\psi + E\sin(c\psi + \alpha). \quad (6)$$

The offset, which was about 10% of the modulation amplitudes, was found in the amplitude signals. Supposing that

$$C/2BJ_2(2\rho_0) = D/2BJ_1(2\rho_0) = 0.1, \quad (7)$$

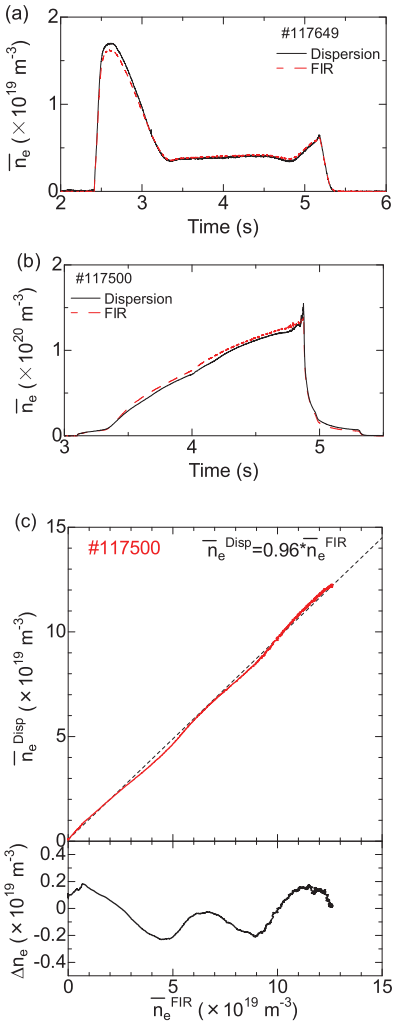

FIG. 6. (a) and (b) Measurement results of low and high density plasmas with the dispersion interferometer n_e^{Dis} and with the far infrared laser interferometer n_e^{FIR}. (c) Comparison between n_e^{Dis} and n_e^{FIR}. An oscillation of the electron density $\Delta n_e = n_e^{Dis} - 0.96 \times n_e^{FIR}$ is found.

the expected density modulation calculated with Eq. (6) is $\pm 1 \times 10^{18}$ m^{-3}, which is close to the measurement results. One of the possible reasons of the offset in the modulation amplitudes is the multi-reflection inside the optical element in the PEM. The multi-reflected lights interfere with each other and the amplitudes of the interference signal will be modulated with the harmonics of the drive frequencies due to slight changes in the thickness of the optical element or change in the refractivity. In order to reduce the offsets, optimization of the incident angle of the laser beam to the PEM to minimize the multi-reflections may be effective.

The fringe jump errors occur easily in the high density range because of fast density change or beam refraction in a plasma. Since there is no density limit such as the Greenwald density in tokamaks, the high density larger than 1×10^{20} m^{-3}, which is comparable to that in ITER standard operation, can be available on LHD. Hence, LHD is a good test platform for robust density measurements. Figure 7 shows measurement results of the high density discharge up to 1.5×10^{20} m^{-3} sustained by repetitive pellets injection. While a fringe jump error occurred in the

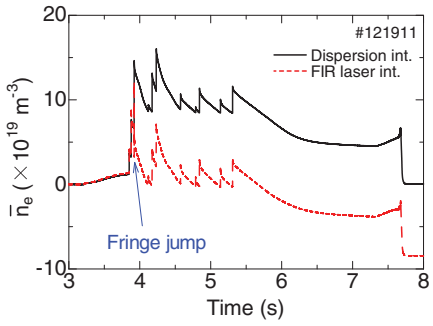

FIG. 7. The temporal evolutions of the line averaged electron density measured with the dispersion interferometer and the far infrared laser interferometer. The fringe jump error occurs at $t = 3.92$ s, as shown by an arrow.

far infrared laser interferometer due to decrease in the detected intensity by beam refraction, the DI can continue measurement. The decrease in the detected intensity was not significant due to shorter wavelength and the DI could track a fast density change of 7.8×10^{20} m^{-3}, which corresponds to 1.8 fringe, during 1 ms by a sampling rate of 100 kHz and with a time constant of lock-in amplifier of 30 μs.

V. DISCUSSION

To be free from fringe jump errors, the expected phase shift should be smaller than 2π. Although there were no fringe jump errors in the pellet injected discharge by the sufficient sampling frequency and the time constant, there still remains the risk of fringe jump errors for the CO_2 laser DI principally because the phase shift is larger than one fringe. A Nd:YAG laser, whose wavelength is 1.064 μm can reduce the phase shift down to 1/10 compared with that of the CO_2 laser. The line density which corresponds to 2π is 1.4×10^{21} m^{-2} for Nd:YAG laser. In case of LHD (optical path length is 3.28 m in double path), even 3×10^{20} m^{-3} which is the maximum line averaged electron density so far, the phase shift is 0.58 fringe and the density can be determined without ambiguity of 2π.

The Nd:YAG laser DI can be composed of commercial optical components. There is a continuous wave Nd:YAG laser with a power of more than 1 W. There are varieties of nonlinear crystals and PPMgSLT has a high conversion efficiency. Combined with the above laser whose output power is 8 W, the second harmonic beam with a power of 2 W will be obtained with PPMgSLT. A high sensitivity detector for the second harmonics is available and about 1 mW is enough for detection. However, 1 μm laser beam is easily attenuated by the surface roughness of the in-vessel mirrors, which is caused by sputtering and depositions of impurities. The reflectivity at the visible light decreased down to less than 10%[18] on LHD, two-three orders higher power is preferable. As for the phase modulator, not only the PEM but also an electro-optic modulator (EOM) is available in this wavelength range, whose drive frequency is higher (e.g., 1 MHz) than that for the PEM. Hence, a faster time response can be expected. One of the concerns is the smaller signal to noise ratio (SNR). This is because the phase shift due to a plasma becomes one order smaller and that due to the vibrations becomes one order larger. In addition to that, the wavefront distortion would be more serious than that for the CO_2 laser. The bench-testing for the examination of SNR of the Nd:YAG laser DI is proceeding in NIFS at present.

VI. SUMMARY

A CO_2 laser (10.6 μm) DI which uses a ratio of modulation amplitudes for phase extraction has been developed on LHD. The DI can improve a limitation of an interferometer: measurement errors due to mechanical vibrations. The original DI suffers from the variations of the detected intensities. The proposed phase extraction method which uses the ratio of modulation amplitudes makes the DI free from the variations of the detected intensities. Hence, the developing DI on LHD is robust against both the mechanical vibrations and the intensity variations.

The phase variations of the DI on LHD are within $\pm 2 \times 10^{17}$ m^{-3} for 3 s without a vibration isolation system on the optical bench. The drift of the baseline is about 5×10^{17} m^{-3} for 30 min. The measurement results of the DI show good agreement with the existing far infrared laser interferometer. The average difference between them of about 5% might come from the evaluation error of the optical path length. The fake density modulation with an amplitude of $\pm 2 \times 10^{18}$ m^{-3} was found during the density ramp-up. The density modulation seems to be attributed to offsets in the amplitudes of modulation components, which are used for the phase evaluations. Since the multi-reflections inside the phase modulator are one of the candidates for what causes the offset, fine adjustment of the incident angle of the probe beam to the modulator would improve the density modulation. In the case of the sufficient sampling rate and time constant of the lock-in amplifiers for amplitude detection of the modulation signal, there is no fringe jump error even in the high density plasma around 1.5×10^{20} m^{-3} sustained by repetitive pellet injections.

For future robust density measurement, a shorter wavelength DI, which adopts a Nd:YAG laser (1.064 μm), can be free from the fringe jump error. The system will be composed by commercial components. The bench-testing for evaluations of signal to noise ratio of the Nd:YAG laser DI which uses the above phase extraction method is in operation.

[1] Y. Kawano, S. Chiba, and A. Inoue, Rev. Sci. Instrum. **72**, 1068 (2001).
[2] H. K. Park, C. W. Domier, W. R. Geck, and N. C. Luhmann, Jr., Rev. Sci. Instrum. **70**, 710 (1999).
[3] T. Akiyama, S. Tsuji-Iio, R. Shimada, K. Nakayama, S. Okajima, M. Takahashi, K. Terai, K. Tanaka, T. Tokuzawa, and K. Kawahata, Rev. Sci. Instrum. **74**, 2695 (2003)
[4] Ch. Fuchs and H. J. Hartfuss, Phys. Rev. Lett. **81**, 1626 (1998).
[5] T. Akiyama, K. Kawahata, Y. Ito, S. Okajima, K. Nakayama, S. Okamura, K. Matsuoka, M. Isobe, S. Nishimura, C. Suzuki *et al.*, Rev. Sci. Instrum. **77**, 10F118 (2006).
[6] F. A. Hopf, A. Tomita, and G. Al-Jumaily, Opt. Lett. **5**, 386 (1980).
[7] Kh. P. Alum, Yu. V. Koval'chuk, and G. V. Ostrovskaya, Sov. Tech. Phys. Lett. **7**, 581 (1981).
[8] V. P. Drachev, Yu. I. Krasnikov, and P. A. Bagryansky, Rev. Sci. Instrum. **64**, 1010 (1993).
[9] P. A. Bagryansky, A. D. Khilchenko, A. N. Kvashnin *et al.*, Rev. Sci. Instrum. **77**, 053501 (2006).
[10] F. Brandi and F. Giammanco, Opt. Lett. **32**, 2327 (2007).

[11]A. Lizunov, P. Bagryansky, A. Khilchenko *et al.*, Rev. Sci. Instrum. **79**, 10E708 (2008).
[12]T. Akiyama, K. Kawahata, S. Okajima, and K. Nakayama, Plasma Fusion Res. **5**, S1041 (2010).
[13]T. Akiyama, K. Kawahata, R. Yasuhara, S. Okajima, and K. Nakayama, J. Instrum. **7**, C01055 (2012).
[14]P. Kornejew, H. Dreier, A. Solomakhin, and M. Hirsch, in *Proceedings if the 39th EPS Conference on Plasma Physics*, Stockholm, 2012, p. P5037, available online at ocs.ciemat.es/epsicpp2012pap/pdf/P5.037.pdf.
[15]D. J. Bamford, E. A. Cummings, D. Panasenko, D. B. Fenner, J. M. Hensley, R. L. Boivin, T. N. Carlstrom, and M. A. Van Zeeland, Rev. Sci. Instrum. **84**, 093502 (2013).
[16]K. Urabe, T. Akiyama, and K. Terashima, J. Phys. D **47**, 262001 (2014).
[17]Y. Shi, Rev. Sci. Instrum. **77**, 036111 (2006).
[18]T. Akiyama, K. Kawahata, N. Ashikawa, M. Tokitani, S. Okajima, K. Nakayama, N. Yoshida, A. Ebihara, K. Tokunaga, Y. Ohtawa, and S. Tsuji-Iio, Rev. Sci. Instrum. **78**, 103501 (2007).